J. Phys. Chem. Solids Vol. 46, No. 4, pp. 437–443, 1985
Printed in the U.S.A.

0022-3697/85 $3.00 + .00

FAR-INFRARED REFLECTION SPECTRA, TO- AND LO-PHONON FREQUENCIES, COUPLED AND DECOUPLED PLASMON-PHONON MODES, DIELECTRIC CONSTANTS, AND EFFECTIVE DYNAMICAL CHARGES OF MANGANESE, IRON, AND PLATINUM GROUP PYRITE TYPE COMPOUNDS†

H. D. LUTZ, G. SCHNEIDER and G. KLICHE
Universität Siegen, Laboratorium für Anorganische Chemie, D-5900 Siegen,
Federal Republic of Germany

(*Received* 17 *February* 1984; *accepted* 2 *August* 1984)

Abstract—The far-infrared reflection spectra of hot-pressed samples of the pyrites MX_2 with M = Mn, Fe, Ru, and Os and X = S, Se, and Te and PtY_2 with Y = P, As, and Sb are presented in the range from 40 to 700 cm^{-1}. The spectra show five reststrahlen bands and more or less free carrier contributions due to deviation from stoichiometry. The oscillator parameters ω_j, ρ_j, γ_j, ω_p, and γ_0, the transverse optical phonon frequencies ω_{TO}, and the coupled plasmon-phonon frequencies Ω_+ and Ω_- were calculated. The uncoupled longitudinal optical phonon frequencies ω_{LO} were determined from $-\mathrm{Im}(1/\hat{\epsilon})$ of the plasmon-free phonon spectra calculated from the oscillator parameters, neglecting the free carrier contributions. The obtained effective ionic charges (Szigeti charges) reveal an increasing covalency of the pyrites in the order pnictides > chalcides and Fe > Ru > Os > Mn compounds. The phonon frequencies reflect the increasing bond strengths on going from 3*d* to 4*d* and 5*d* metal compounds, discussed in a former work (*Phys. Chem. Miner.* **9**, 109 (1983)). The true intensities of the phonon modes for using them with respect to lattice dynamical calculations are discussed.

INTRODUCTION

From the far-infrared reflection spectra of semiconducting compounds a lot of physical properties can be derived which are of interest for solid state scientists, e.g. optical and dielectric constants, the transverse optical (TO) and longitudinal optical (LO) phonon frequencies, effective dynamical ionic charges and, in appropriate cases, the free carrier plasma frequencies. This is done by the Kramers–Kronig analysis or by oscillator-fit methods. For lattice dynamical calculations on pyrite-type chalcides and pnictides [1], we needed the oscillator parameters, especially the TO and LO phonon frequencies, of these compounds.

From previous studies only few data of FeS_2 [2–4], MnS_2 [4, 5], $MnSe_2$ [4, 6, 7], and $MnTe_2$ [4, 6, 7] are available, obtained from natural single crystals [2–5], and from synthetic materials [4, 6, 7]. Apart from infrared absorption spectra of polycrystalline samples [8], no data on platinum group metal pyrites are reported. In this article we therefore studied the far-infrared reflection spectra, the phonon frequencies, and the optical and dielectric constants of the pyrites RuS_2, $RuSe_2$, $RuTe_2$, OsS_2, $OsSe_2$, $OsTe_2$, PtP_2, $PtAs_2$, and $PtSb_2$.

† Lattice vibration spectra, Part XXXV, Part XXXIV, Lutz H. D., Henning J., Buchmeier W. and Engelen B., *J. Raman Spectrosc.* **15**, 336 (1984).

Because of the lack of suitable single crystals, hot-pressed polished samples with mirror-like surfaces must be used for the reflectivity measurements. As discussed in Ref. [4], from the spectra of specimens pressed at room temperature the true phonon frequencies, but not large enough values of the permittivities ϵ_0 and ϵ_∞, can be computed because of the reduced reflectivity compared to single crystal measurements. Using hot-pressed pellets, however, more accurate dielectric constants can be obtained [9] because of the higher surface quality compared to cold-pressed samples, see Refs. [1, 9].

All platinum metal group pyrites show free carrier contributions in addition to the phonon modes in the far-infrared spectra. This prohibits direct determination of the LO phonon mode frequencies from the observed reflectivity by means of the Kramers–Kronig analysis. Coupled Ω_+ and Ω_- frequencies, due to coupling of the plasmons with the longitudinal optical phonons, are obtained instead of the pure LO frequencies and the plasma resonance frequency ω_p' [10]. Even very small free carrier concentrations shift the Ω_+ frequencies away from the true LO modes by some wavenumbers [1]. We therefore tried to fit the recorded reflection spectra very carefully by oscillator model calculations in order to decouple the modes to obtain the pure LO frequencies from the plasmon-free spectra of the pyrites under investigation.

EXPERIMENTAL

The pyrites $MnSe_2$, $MnTe_2$, FeS_2, RuS_2, $RuSe_2$, $RuTe_2$, OsS_2, $OsSe_2$, $OsTe_2$, PtP_2, $PtAs_2$, and $PtSb_2$ were prepared by annealing stoichiometric mixtures of the elements in evacuated quartz tubes at temperatures of about 500–900°C for about 14 days (see Table 1), X-ray powder methods were used to confirm the structure and the lattice constants of the compounds. Suitable pellets of the pyrite samples for the reflectivity measurements were obtained by hot-pressing in a graphite die at 100–200 MPa and 350–800°C (see Table 1) and polishing with diamond paste (0.5 μm).

Measurements of the far-infrared reflection spectra were performed at near normal incidence using a Bruker IFS 114 Fourier-transform interferometer in the spectral range from 30–700 cm^{-1} (resolution < 2 cm^{-1}). An aluminum mirror was used as reference.

FAR-INFRARED REFLECTION SPECTRA

Pyrites crystallize in the cubic space group $Pa3/T_h^6$, $Z = 4$. Unit cell group analysis predicts five infrared active modes of species F_u. Figure 1 shows the far-infrared reflection spectra of the pyrites under investigation.

The five group theoretically allowed modes are observed in the spectra of all pyrites studied, even in the case of $MnTe_2$, for which in the previous article [4] only three reststrahlen bands were found. In the case of $RuTe_2$, both a 5 and a 6 phonon mode fit is possible (see Table 2). The latter fit with the highest wavenumbered reststrahlen band at 257 cm^{-1} would be expected, comparing the spectra with those of the isotypic RuS_2 and $RuSe_2$, but then one of the five other bands must be superfluous, presumably the band at 222 cm^{-1}. Lattice dynamical calculations [1], however, indicate that the band at 257 cm^{-1} does not belong to the five infrared active lattice modes. Such superfluous reststrahlen bands are claimed, in the literature, to be surface defect modes or donor and acceptor modes, respectively [11, 12]. The spectra of different preparations and different pellets of one preparation differ to some extent, a shown for RuS_2 [1]. This is due to the different surface quality of the pellets and the different concentrations of free carriers.

The presence of free carriers is shown by the increased reflectivity in the low-wavenumber region of the spectra. In the case of large free carrier contributions, e.g. for $PtSb_2$ (see Fig. 1), the phonon modes are hidden by the plasma band. No free carriers are found in MnS_2, $MnSe_2$, $MnTe_2$, and FeS_2 [4].

OSCILLATOR-FIT CALCULATIONS

From the observed far-infrared reflection spectra the optical and dielectric constants are calculated using the classical oscillator model with a Drude term included to take account of free carrier contributions. The reflectivity R of a sample

$$R = \left[\frac{\hat{\epsilon}^{1/2} - 1}{\hat{\epsilon}^{1/2} + 1}\right]^2$$

is calculated from the dielectric function

$$\hat{\epsilon} = \epsilon_\infty + \hat{\epsilon}_{vib} + \hat{\epsilon}_{fc}$$

where ϵ_∞ is the high-frequency dielectric constant, $\hat{\epsilon}_{vib}$ the contribution of the lattice vibrations to the dielectric constant

$$\hat{\epsilon}_{vib} = \sum_{j=1}^{n} \frac{4\pi\rho_j\omega_j^2}{(\omega_j^2 - \omega^2) - i\,\gamma_j\omega}$$

(n is the number of oscillators, ρ_j the oscillator

Table 1. Preparation and hot-pressing of manganese, iron, and platinum group pyrites

	Preparation temperature (°C)	Annealing time (days)	Hot-pressing temperature (°C)	Time of hot-pressing (hrs)
$MnSe_2$	380	14	350	8
$MnTe_2$	600	14	550	8
FeS_2	400	14	450	16
RuS_2	800-900	14	800	8
$RuSe_2$	800-900	14	800	8
$RuTe_2$	800-900	14	800	8
OsS_2	800-900	14	800	10
$OsSe_2$	800-900	14	800	8
$OsTe_2$	800	10	750	10
PtP_2	500	14	450	10
$PtAs_2$	600	10	550	8
$PtSb_2$	600	14	500	8

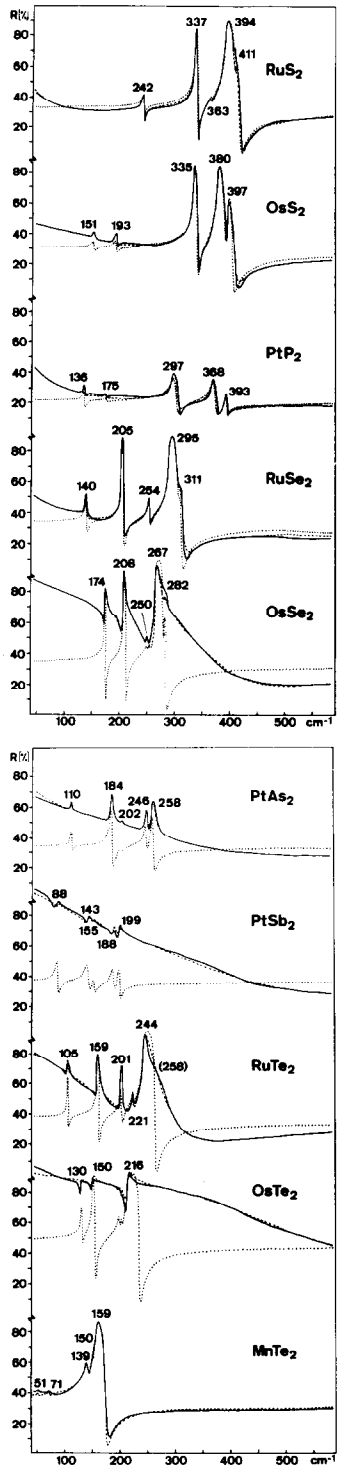

Fig. 1. Far-infrared reflection spectra of $MnTe_2$ and platinum group pyrites (dashed lines, oscillator-fit calculations; dotted lines, plasmon-free spectra, see text). Given frequencies, maxima of the reststrahlen bands.

strength, ω_j the eigenfrequency, and γ_j the damping of oscillator j), $\hat{\epsilon}_{fc}$ is the free carrier contribution

$$\hat{\epsilon}_{fc} = -\frac{\omega_p^2}{\omega(\omega + i\,\gamma_0)}$$

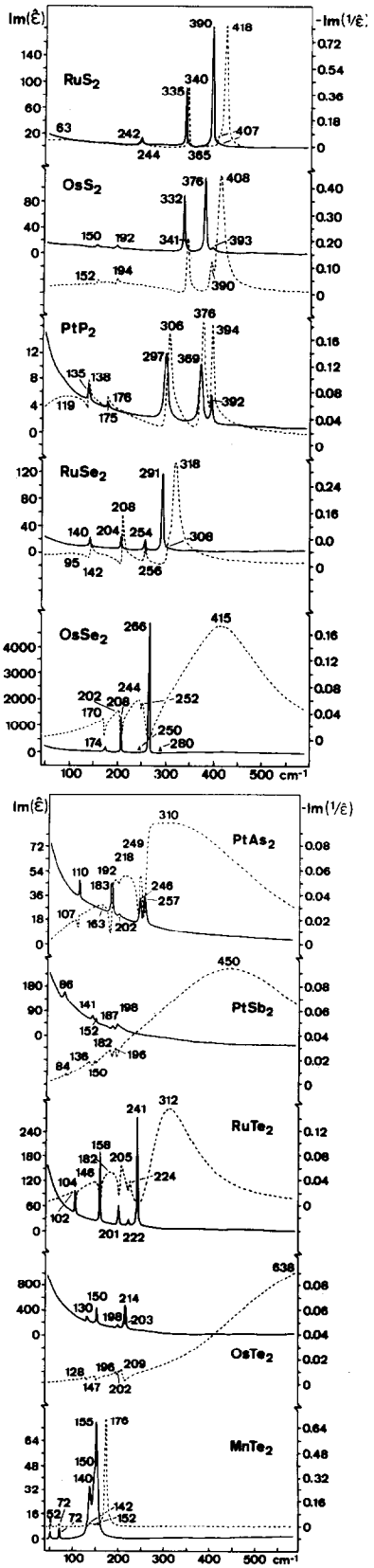

Fig. 2. Dispersion functions of the dielectric constants of $MnTe_2$ and platinum group pyrites calculated by oscillator-fit method: ——, $\mathrm{Im}(\hat{\epsilon})$; – – –, $-\mathrm{Im}(1/\hat{\epsilon})$. Given frequencies, maxima of the dispersion functions, i.e. ω_{TO} and $\Omega_{\pm}$ (or ω_{LO}), respectively.

Table 2. Oscillator parameters, TO and LO phonon frequencies, plasma frequencies (cm^{-1}), and effective charges[a] of manganese, iron, and platinum group pyrites

	j	ω_j[b]	$4\pi p_j$[b]	γ_j[b]	ω_{TO}[c]	ω_{LO}[c]	ω_{abs}[d]	plasmons[f]
MnS_2[e]								
ε_∞ =5.36[b]	1	254	0.43	21.36	252	275	258	
ε_0 =8.11[b]	2	224	0.64	12.77	221	237	228	
Z_e^*/e=0.84	3	193	1.36	12.45	193	204	198	
e_B^*/e=2.08	4	131	0.26	3.39	129	132	131	
e_S^*/e=0.84	5	90	0.07	1.48	91	92	90	
$MnSe_2$[e]								
ε_∞ =8.34	1	180	2.43	15.98	180	211	187	
ε_0 =12.38	2	170	0.26	3.81	170	174	171	
Z_e^*/e=0.91	3	162	1.16	3.92	160	166	164	
e_B^*/e=2.62	4	94	0.13	0.89	94	95	94	
e_S^*/e=0.76	5	66	0.06	0.73	68	69	69	
$MnTe_2$[e]								
ε_∞ =12.74	1	155	1.72	3.16	155	176	161	
ε_0 =17.55	2	150	1.51	6.75	150	152	150	
Z_e^*/e=0.81	3	140	1.51	6.63	140	142	140	
e_B^*/e=2.90	4	72	0.05	0.54	72	72	74	
e_S^*/e=0.59	5	52	0.03	0.26	52	52		
FeS_2[e]								
ε_∞ =19.80	1	422	0.01	10.04	422	439	433	
ε_0 =24.11	2	412	0.33	13.93	412	421	416	
Z_e^*/e=0.90	3	401	3.21	3.97	401	411	398	
e_B^*/e=4.17	4	348	0.42	0.83	348	350	349	
e_S^*/e=0.60	5	293	0.34	2.78	293	294	293	
RuS_2								
ε_∞ =11.56	1	407	0.06	7.65	407	417	405	ω_p' = 110
ε_0 =13.62	2	390	1.30	2.69	390	406	391	ω_p = 406
Z_e^*/e=0.95	3	365	0.02	3.65	365	365	365	γ_0 = 220
e_B^*/e=3.23	4	335	0.56	1.24	335	340	340	
e_S^*/e=0.71	5	242	0.11	2.64	242	243	244	

[a] Effective dynamical charges; 'normalized splittings', Ze^*/e ($=S^{1/2}$); transverse charges, e_B^*/e; Szigeti charges, e_S^*/e (see Ref. [9]).

[b] From oscillator fit method, ω_j, γ_j (cm^{-1}).

[c] From $\mathrm{Im}(\hat{\varepsilon})$ and $-\mathrm{Im}(1/\hat{\varepsilon})$ of the plasmon-free spectra, oscillator-fit (see text).

[d] From infrared absorption spectra of polycrystalline samples, literature data see Refs. [4, 8] and the references cited therein.

[e] Literature data see Ref. [4].

[f] Plasma frequency, ω_p, plasma resonance frequency, ω_p', and damping of the free carriers, γ_0, (cm^{-1}); from oscillator fit.

[g] Additional oscillator necessary to fit the obtained spectra, which is obviously also due to the free carriers (see text).

with the plasma frequency

$$\omega_p^2 = \frac{4\pi e^2 n_0}{m^*} = \omega_p'^2 \cdot \epsilon_1$$

(n_0 is the number of free carriers, γ_0 the damping, m^* the effective mass of the free carriers, ω_p' the plasma resonance frequency, and ϵ_1 the effective dielectric constant).

In most cases it was possible to fit the reflection spectra of the pyrites under investigation using appropriate oscillator parameters. The calculated spectra are given in Fig. 1 (dashed lines). For the oscillator parameters ω_j, ρ_j, γ_j, ω_p, γ_0, ϵ_∞, and ϵ_0, see Table 2. In some cases an additional phonon-like oscillator with very large damping, e.g. for OsS_2, $RuSe_2$, $RuTe_2$, and $PtAs_2$, or a second plasmon with different damping constant γ_0, e.g. for $OsSe_2$, $OsTe_2$, $PtAs_2$, and

Table 2. (*Continued*)

	j	ω_j[b]	$4\pi\rho_j$[b]	γ_j[b]	ω_{TO}[c]	ω_{LO}[c]	ω_{abs}[d]	plasmons[f]	
OsS_2									
ε_∞ =10.38	1	393	0.13	5.50	393	404	399	ω_p' = 111	
ε_0 =12.44	2	376	1.03	3.20	376	390	389	ω_p = 390	
Z_e^*/e=1.06	3	333	0.72	1.43	332	340	339	γ_0 = 285	
e_B^*/e=3.34	4	192	0.09	3.69	192	193	193		
e_S^*/e=0.81	5	151	0.08	3.04	150	152	150		
	6[g]	150	5.65	120					
PtP_2									
ε_∞ =7.1	1	392	0.03	2.19	392	393	393	ω_p' = 244	
ε_0 =7.66	2	369	0.17	7.22	369	374	372	ω_p = 675	
Z_e^*/e=0.63	3	297	0.28	8.02	297	302	303	γ_0 = 700	
e_B^*/e=1.67	4	175	0.02	2.98	175	176	175		
e_S^*/e=0.55	5	135	0.06	1.96	135	136	137		
$RuSe_2$									
ε_∞ =11.96	1	308	0.05	6.30	308	314	308	ω_p' = 70	
ε_0 =14.60	2	291	1.63	2.30	291	307	300	ω_p = 265	
Z_e^*/e=1.04	3	254	0.15	2.16	254	256	255	γ_0 = 77	
e_B^*/e=3.60	4	205	0.53	0.20	204	208	208		
e_S^*/e=0.77	5	140	0.28	2.49	140	142	141		
	6[g]	166	14.45	393					
$OsSe_2$									
ε_∞ =12.50	1	280	0.03	2.66	280	284	282	ω_p' = 380	174
ε_0 =15.00	2	266	1.48	0.08	266	279	264	ω_p =1345	674
Z_e^*/e=1.04	3	250	0.04	1.75	250	250	248	γ_0 = 300	50
e_B^*/e=3.68	4	208	0.56	0.08	208	212	212		
e_S^*/e=0.76	5	174	0.38	0.35	174	176	178		
$PtAs_2$									
ε_∞ =13.5	1	257	0.40	4.11	257	262	262	ω_p' = 391	
ε_0 =14.7	2	246	0.17	2.36	246	248	246	ω_p =1435	
Z_e^*/e=0.66	3	202	0.03	3.15	202	202	204	γ_0 = 603	
e_B^*/e=2.42	4	183	0.50	2.56	183	186	186		
e_S^*/e=0.47	5	110	0.10	0.81	110	110	111		
	6[g]	196	5.84	236					

$PtSb_2$ (see Table 2), must be included to fit the steep ascent of the low-wavenumbered reflectivity.

The TO and LO phonon frequencies were determined from the maxima of the dispersion functions $\mathrm{Im}(\hat{\varepsilon})$, and $-\mathrm{Im}(1/\hat{\varepsilon})$, respectively [9] (see Fig. 2). In the presence of free carrier contributions, however, by this means only the coupled Ω_+ and Ω_- plasmon-LO-phonon frequencies [13]

$$\Omega_\pm^2 = \frac{1}{2}(\omega_p'^2 + \omega_{LO}^2) \pm \frac{1}{2}\left[(\omega_p'^2 - \omega_{LO}^2)^2 + 4\omega_p'^2\omega_{LO}^2\left(1 - \frac{\epsilon_\infty}{\epsilon_0}\right)\right]^{1/2}$$

are obtained instead of the LO phonon frequencies and the plasma resonance frequencies ω_p'. The TO phonon frequencies are not affected by the longitudinal plasma modes. The uncoupled LO phonon frequencies were determined from the dispersion function $-\mathrm{Im}(1/\hat{\varepsilon})$ calculated without the plasmon contributions (see Fig. 3). (Calculation of the uncoupled LO frequencies from the TO frequencies and the oscillator strengths, as reported by Iishi [14], is only possible in the one-oscillator case [1].) In a similar manner, we calculated the plasma-free reflection spectra (see Fig. 1) by substracting the free carrier contributions from the experimental spectra, using the oscillator parameters ω_p, γ_0, etc. The obtained phonon frequencies (and the dynamical effective ionic charges e_s^*/e, e_B^*/e, and Ze^*/e, for details see Ref. [9]) are included in Table 2. The given frequencies have an uncertainty of ± 2 cm^{-1}, excepting the compounds with large free carrier contributions. The

Table 2. (*Continued*)

	j	ω_j [b]	$4\pi\rho_j$ [b]	γ_j [b]	ω_{TO} [c]	ω_{LO} [c]	ω_{abs} [d]	plasmons [f]	
$RuTe_2$									
ε_∞ =14.04	1	242	2.51	1.69	241	264	257	ω_p' = 291	
ε_0 =17.84	1'	257	0.27	14.13	257	267		ω_p =1090	
Z_e^*/e=1.11	1''	242	2.26	1.45	242	256	241	γ_0 = 244	
e_B^*/e=4.18	2	222	0.13	1.84	222	223	222		
e_S^*/e=0.78	2'	222	0.15	2.09	222	223			
	3	201	0.25	0.56	201	202	201		
	4	158	0.65	0.60	158	161	160		
	5	104	0.25	0.47	104	105	105		
	6[g]	42	39.60	34.60					
$OsTe_2$									
ε_∞ =24.00	1	214	4.59	2.57	214	236		ω_p' = 513	260
ε_0 =31.80	2	203	0.17	1.62	203	204		ω_p =2515	1273
Z_e^*/e=1.35	3	198	0.21	0.99	198	199		γ_0 = 179	202
e_B^*/e=6.6	4	150	2.32	1.28	150	155			
e_S^*/e=0.76	5	130	0.51	0.69	130	131			
$PtSb_2$									
ε_∞ =15.70	1	198	0.18	2.42	198	200		ω_p' = 217	497
ε_0 =17.50	2	187	0.25	3.74	187	188		ω_p = 859	1969
Z_e^*/e=0.77	3	152	0.14	2.89	152	158		γ_0 = 9	562
e_B^*/e=3.07	4	141	0.63	5.64	141	144			
e_S^*/e=0.52	5	86	0.63	2.58	86	88			

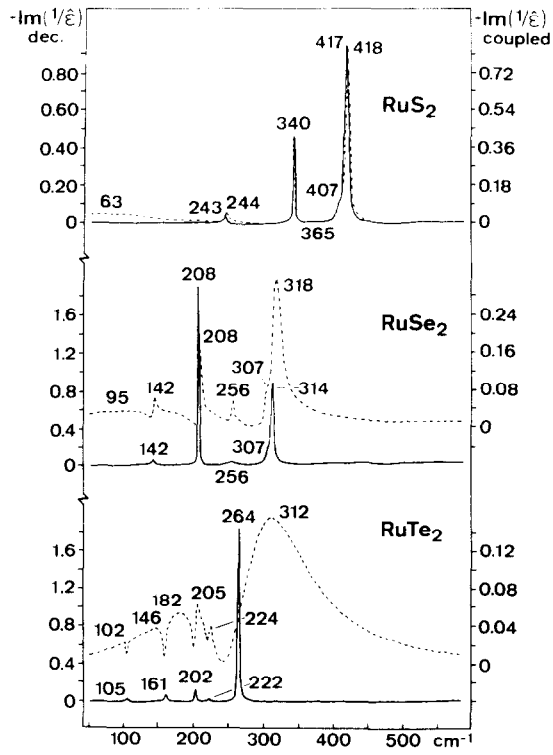

Fig. 3. Dispersion functions $-\mathrm{Im}(1/\hat{\varepsilon})$ of the pyrites RuS_2, $RuSe_2$, and $RuTe_2$: – – –, plasmon included (coupled); ——, without plasmon contributions (decoupled). Given frequencies, maxima of the dispersions functions, i.e. Ω_+ and ω_{LO}, respectively.

uncertainty of the oscillator parameters ρ_j, γ_j, ε_∞, etc., may be somewhat higher because their values depend strongly on the surface quality of the pellets used, i.e. the absolute reflectivity.

DISCUSSION

The phonon frequencies of the manganese, iron, and platinum group pyrites are as discussed recently [15]. Thus the so-called Plendl frequencies $\bar{f}$ obtained from the mean intensity weighted frequencies $\bar{\nu}$ [16] increase on going from 3*d* to 5*d* metals and decrease on going from lighter to heavier non-metal atoms and on going from chalcides to pnictides. (The Plendl frequencies given in Table 3 are calculated using the TO frequencies and oscillator strengths of the reststrahlen bands instead of the peak frequencies and peak intensities of usual infrared absorption spectra [15].)

The effective ionic charges (Szigeti charges), which can be determined from the TO/LO splittings (for details see Ref. [9]), and, hence, the ionicities of the manganese, iron, and platinum group pyrites, are as expected from common chemical sense (see Fig. 4), i.e. they decrease in the order sulfides > selenides > tellurides, chalcides > pnictides, Mn > Os > Ru > Fe compounds. Conspicuous, but also due to the reduced ionicity, are the much smaller oscillator strengths and reflectivities of the reststrahlen bands of the platinum pnictides compared to those of the ruthenium and osmium chalcides (see Fig. 1 and

Table 3. Oscillator strength weighted, $\bar{\nu}$ [cm^{-1}], and mass weighted, $\bar{f}$ [N cm^{-1}], mean TO phonon frequencies of pyrite type compounds

	$\bar{\nu}$	$\bar{f}$
MnS_2	202	0.71
$MnSe_2$	170	0.69
$MnTe_2$	147	0.58
FeS_2	388	2.65
RuS_2	367	3.12
$RuSe_2$	256	2.38
$RuTe_2$	215	1.97
OsS_2	362	3.70
$OsSe_2$	239	2.90
$OsTe_2$	189	2.29
PtP_2	301	2.52
$PtAs_2$	211	2.23
$PtSb_2$	135	1.17

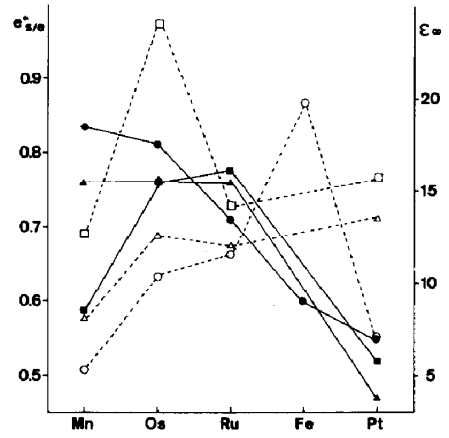

Fig. 4. Szigeti dynamical effective ionic charges e_s^*/e, ●, ▲, ■, and high-frequency dielectric constants, ϵ_∞, ○, △, □, of manganese, iron, and platinum group pyrites: ●, ○, sulfides, phosphides; ▲, △, selenides, arsenides; ■, □, tellurides, antimonides.

Table 2). The dielectric constants ϵ_∞ (see Fig. 4) reveal both the different polarizabilities of the atoms involved and the extent of electron delocalization in the pyrites under discussion.

The observed intensities of the lattice modes in the absorption or reflection spectra (and also the TO/LO splittings) do not reflect the 'inherent' intensities of the individual lattice modes because a transfer of intensity from low-wavenumbered to high-wavenumbered modes takes place, especially in the case of small frequency differences of the modes. The true intensities of the lattice vibrations, given by the obtained oscillator strengths, are shown by the peak intensities of the dispersion function $\mathrm{Im}(\hat{\epsilon})$. Compare, e.g. the 'intensity' of the highest-wavenumbered reststrahlen band of OsS_2 in the reflection spectrum and in the $\mathrm{Im}(\hat{\epsilon})$ curve (Figs. 1 and 2). This possible intensity transfer must be considered by using intensity data as additional (to the frequencies) experimental values for lattice dynamical calculations.

In some cases it was necessary to introduce two plasmon-like contributions different with respect to ω_p and γ_0 or an (free carrier caused?) additional phonon-like contribution in order to fit the observed reflection spectra by oscillator fit methods. The physical significance of more than one plasmon, however, is not clear.

Preliminary studies showed that the plasma frequencies and, hence, the free carrier concentrations of the pyrites studied are not temperature dependent, as found for other semiconductors, see e.g. the skutterudites CoP_3 and $CoAs_3$ [17]. We therefore assume that the free carriers found in the pyrite type chalcides and pnictides are caused by deviation from stoichiometry with fully ionized impurity levels. This is supported by the finding that the obtained plasma frequencies depend on sample preparation, but not on the pellet quality.

Acknowledgements—The authors would like to thank the Deutsche Forschungsgemeinschaft and the Fonds der Chemischen Industrie for financial support.

REFERENCES

1. Schneider G., Dissertation, Siegen (1983).
2. Verble J. L. and Wallis R. F., Phys. Rev. **182**, 783 (1969).
3. Schlegel A. and Wachter P., *J. Phys.* **C9**, 3363 (1976).
4. Lutz H. D., Kliche G. and Haeuseler H., *Z. Naturforsch.* **36a**, 184 (1981).
5. Verble J. L. and Humphrey F. M., *Solid State Commun.* **15**, 1693 (1974).
6. Onari S., Arai T. and Kudo K., *J. Phys. Soc. Japan* **37**, 1585 (1974).
7. Onari S. and Arai T., *J. Phys. Soc. Japan* **46**, 184 (1979).
8. Lutz H. D. and Willich P., *Z. Anorg. Allg. Chem.* **428**, 199 (1977).
9. Lutz H. D., Wäschenbach G., Kliche G. and Haeuseler H., *J. Solid State Chem.* **48**, 196 (1983).
10. Lutz H. D. and Kliche G., *Phys. Stat. Sol (b)* **112**, 549 (1982).
11. Renneke D. R. and Lynch D. W., *Phys. Rev.* **138**, A530 (1965).
12. Barker A. S., *Phys. Rev.* **B7**, 2507 (1973).
13. Olson C. G. and Lynch D. W., *Phys. Rev.* **177**, 1231 (1969).
14. Iishi K., Salje E. and Werneke Ch., *Phys. Chem. Miner.* **4**, 173 (1979).
15. Lutz H. D., Schneider G. and Kliche G., *Phys. Chem. Miner.* **9**, 109 (1983).
16. Plendl J. N., *Phys. Rev.* **123**, 1172 (1961).
17. Kliche G. and Lutz H. D., *Infrared Physics* **24**, 171 (1984).